Chapter 6

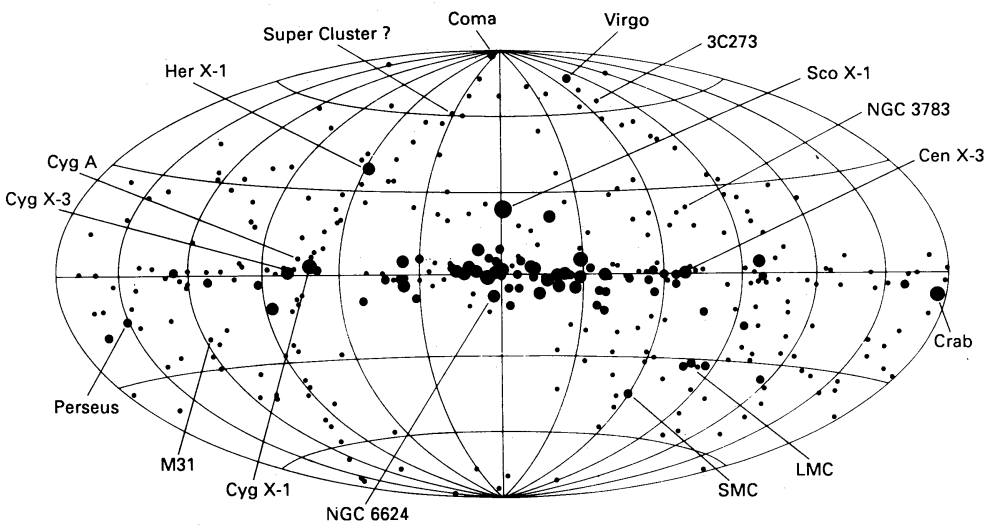
X-ray astronomy

	page
Uhuru X-ray map	184
The HEAO A1 all sky map	185
Galactic sources: binaries and stars	186
Soft X-ray H–R diagrams	188
Binary X-ray pulsars	189
X-ray emitting supernova remnants	191
Crab Nebula	192
X-ray emission from normal galaxies	193
X-ray emission from clusters of galaxies	193
X-ray emission from active galaxies	193
3C 273	194
Quasar X-ray luminosity	195
X-ray source nomogram	196
Diffuse X-ray background	197
Absorption of X-rays	198
Photoabsorption cross-sections (UV–X-ray)	198
Effective cross-section of the interstellar medium	199
Total photo-ionization cross-section	200
Photoelectric absorption cross-section	201
Attenuation of photons in the atmosphere	203
Photoelectric absorption in the interstellar medium	204
Spectral features	204
Model X-ray spectral distributions	205
Emission lines for low density plasma	206
Plasma emission – power in lines	208
Bibliography	208

© Cambridge University Press • Provided by the NASA Astrophysics Data System

Uhuru X-ray map

X-ray sources from the *Fourth Uhuru Catalog* displayed in galactic coordinates. The size of the symbol representing a source is proportional to the logarithm of the peak source intensity. The 339 X-ray sources observed with the UHURU (SAS-A) X-ray observatory are displayed. (Adapted from Forman, W. *et al.*, *Ap. J. Suppl.*, **38**, 357, 1978.)

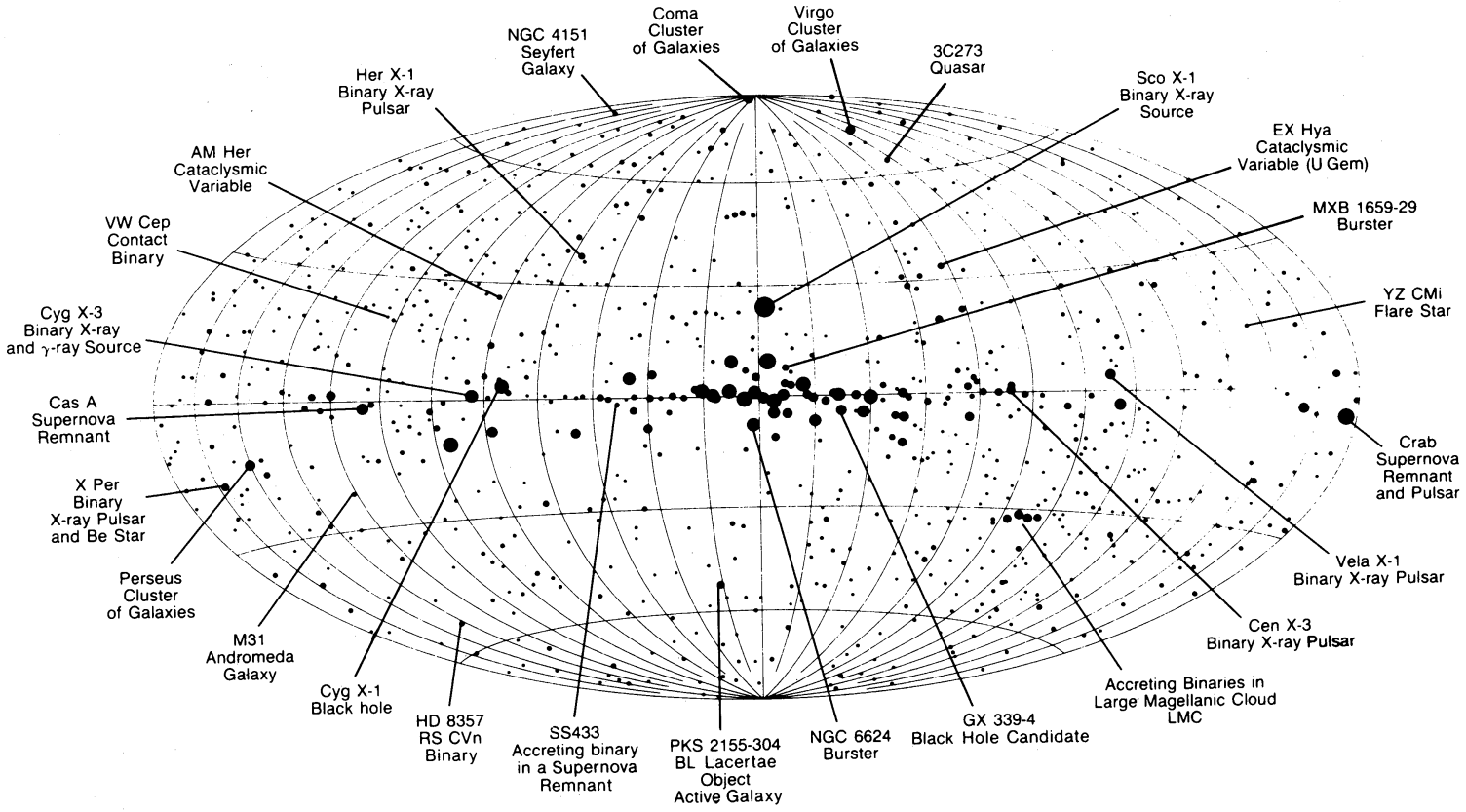


© Cambridge University Press • Provided by the NASA Astrophysics Data System

© Cambridge University Press • Provided by the NASA Astrophysics Data System

The HEAO A1 all sky map

Discrete X-ray sources observed by the NRL Sky Survey Experiment on HEAO-1 are displayed in galactic coordinates. The size of the dot representing a source is proportional to the logarithm of the intensity averaged over the time interval when the source was in the field of view. 700 sources are shown. (Courtesy of K. Wood, Naval Research Laboratory.)



Source	α 1950 δ 1950	Flux density[a] (2–11 keV) max (μJy) min (μJy)	$L(X)$ max (2–11 keV) (erg s^{-1})	V magnitude	$\frac{L(X)}{L(O)}$	Spectral type	Periods	Distance	Remarks
SMC X−1	01^h 15^m 45^s.6 −73° 42′ 22″	57 2	6×10^{38}	13.3	1.2	B0 I	3.89^d 0.71^s	65 kpc	Sanduleak 160
β Per	03 04 54.3 40 45 52	9	2×10^{31}	2.2	5×10^{-5}	B8 V/K0 IV/ Am	2.9^d	32 pc	Algol
3U 0352+30	03 52 15.1 30 54 01	37 11	1.2×10^{34}	6.0–6.7	1×10^{-4}	O9.5 (III–V)e	581^d (?) 13.9^m	350 pc	X Per
A 0620−00	06 20 11.1 −00 19 11	~50 000 ≲5	3×10^{38}	10.4 (18.3)	85			1.5–2.5 kpc	X-ray Nova V616 Mon
Vela X−1	09 00 13.2 −40 21 25	280 <28	1.4×10^{36}	6.9	3×10^{-3}	B0.5 Ib	8.97^d 283^s	1.4 kpc	HD 77581
Cen X−3	11 19 01.9 −60 20 57	224 <21	4×10^{37}	13.4	0.05	O6.5 II–III	2.09^d 4.8^s	8 kpc	Krzeminski's star
Sco X−1	16 17 04.5 −15 31 15	19 000 6900	2×10^{37}	12.2–13.3	600		0.787^d	0.7 kpc	V818 Sco
Her X−1	16 56 01.7 35 25 05	160 11	1.0×10^{37}	13.2	10	A09–F0	34.8^d 1.7^d 1.2^s	5 kpc	HZ Her
3U 1700−37	17 00 32.7 −37 46 29	110 <11	3×10^{36}	6.6	5×10^{-4}	O6.5f	3.4^d	1.7 kpc	
4U 1813+50	18 14 58.6 49 50 55	7 2.5	8×10^{33}	13.1–12.3	0.6		0.129^d	300 kpc	AM Her

© Cambridge University Press • Provided by the NASA Astrophysics Data System

Cyg X−1	19 56 28.9 35 03 55.0	1320 260	2×10^{37}	8.9	2×10^{-2}	O9.7 Iab	5.6[d]	2.5 kpc	Blackhole candidate HDE 226868
Cyg X−3	20 30 37.6 40 47 13	430 90	1.2×10^{38}				16.8[d] (?) 4.8[h]	10.5 kpc	IR/radio
SS Cygni	21 40 42.6 43 21 51	20 5	$1–5 \times 10^{32}$	12.1–8.1	1.3		$6^h\,38^m$	100 pc	Dwarf nova (U Gem)
Cyg X−2	21 42 36.9 38 05 28	740 220		15.5	450		11.2[d]		Sub-dwarf

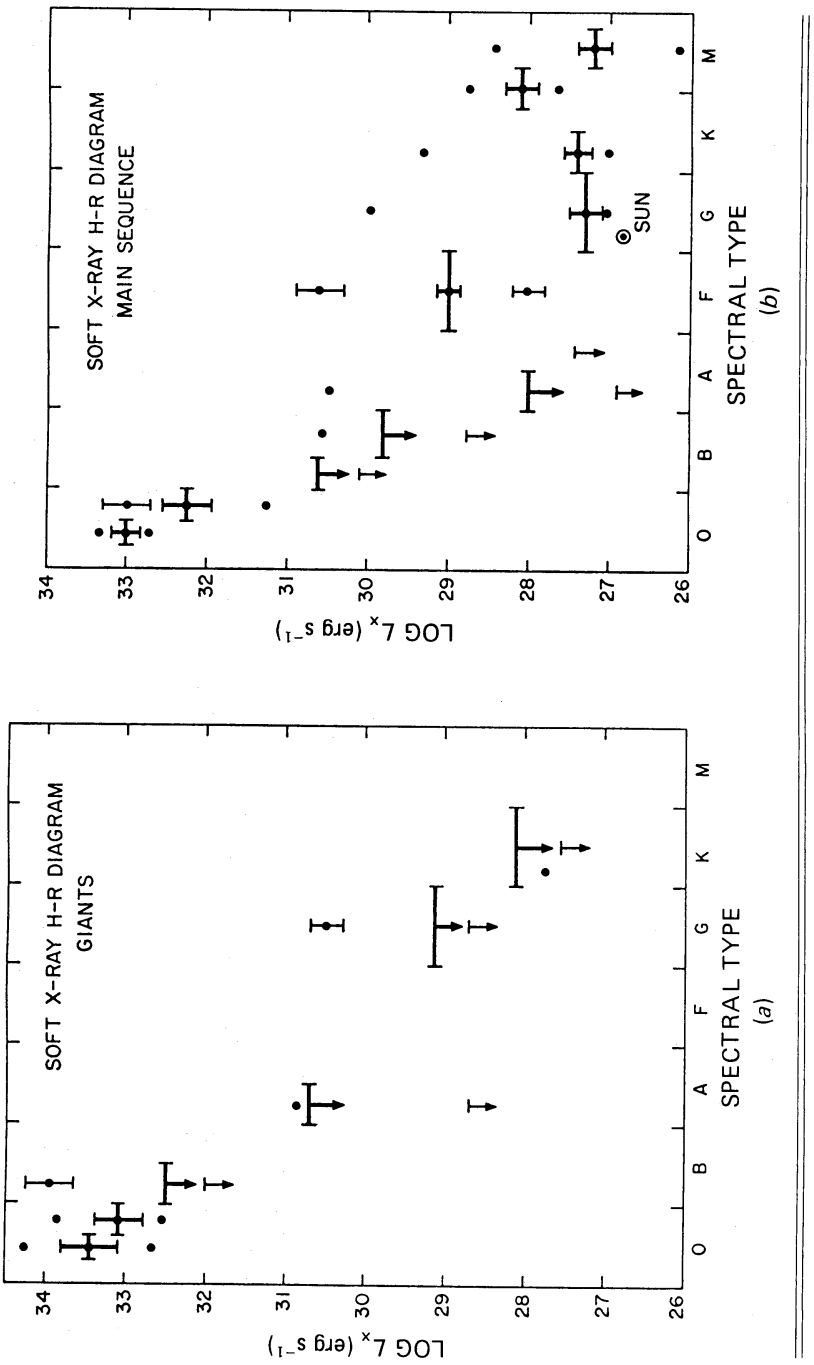
		X-ray intensity (>0.2 keV) (erg cm^{-2} s^{-1})						
UV Cet	1 36 24 −18 13 00	7×10^{-11}	6.8–12.9	2×10^{-3}	dM5.5 e			Flare star
α Aur	5 12 59.5 45 56 58	3×10^{-10}	0.1	1×10^{-5}	G8 III + F	104[d]	14 pc	Capella
α CMa	6 42 54 −16 39 00	9.5×10^{-12}	−1.5		A IV + D0	44.98[y]	2.7 pc	Sirius
HZ 43	13 14 00 29 22 00	9×10^{-10}	12.9	6				White dwarf

[a] Flux density = (integrated 2–11 keV flux)/9 keV; $1\,\mu\text{Jy} = 0.242 \times 10^{-11}$ erg cm^{-2} s^{-1} keV^{-1} $= 1.51 \times 10^{-3}$ keV cm^{-2} s^{-1} keV^{-1}.
(Adapted from Bradt, H. V., Doxsey, R. E. & Jernigan, J. G., *COSPAR Symposium on X-ray Astronomy*, Innsbruck, Austria, May 31, 1978).

© Cambridge University Press • Provided by the NASA Astrophysics Data System

Soft X-ray H–R diagrams

Soft X-ray (0.15–3 keV) H–R diagram for (*a*) giant and (*b*) main sequence stars from the Einstein Observatory stellar survey (K. Topka, thesis, Harvard University, 1980). Thick bars and arrows denote X-ray luminosity medians or their upper limits. The upper limit or lowest detection and the highest detection are also shown.

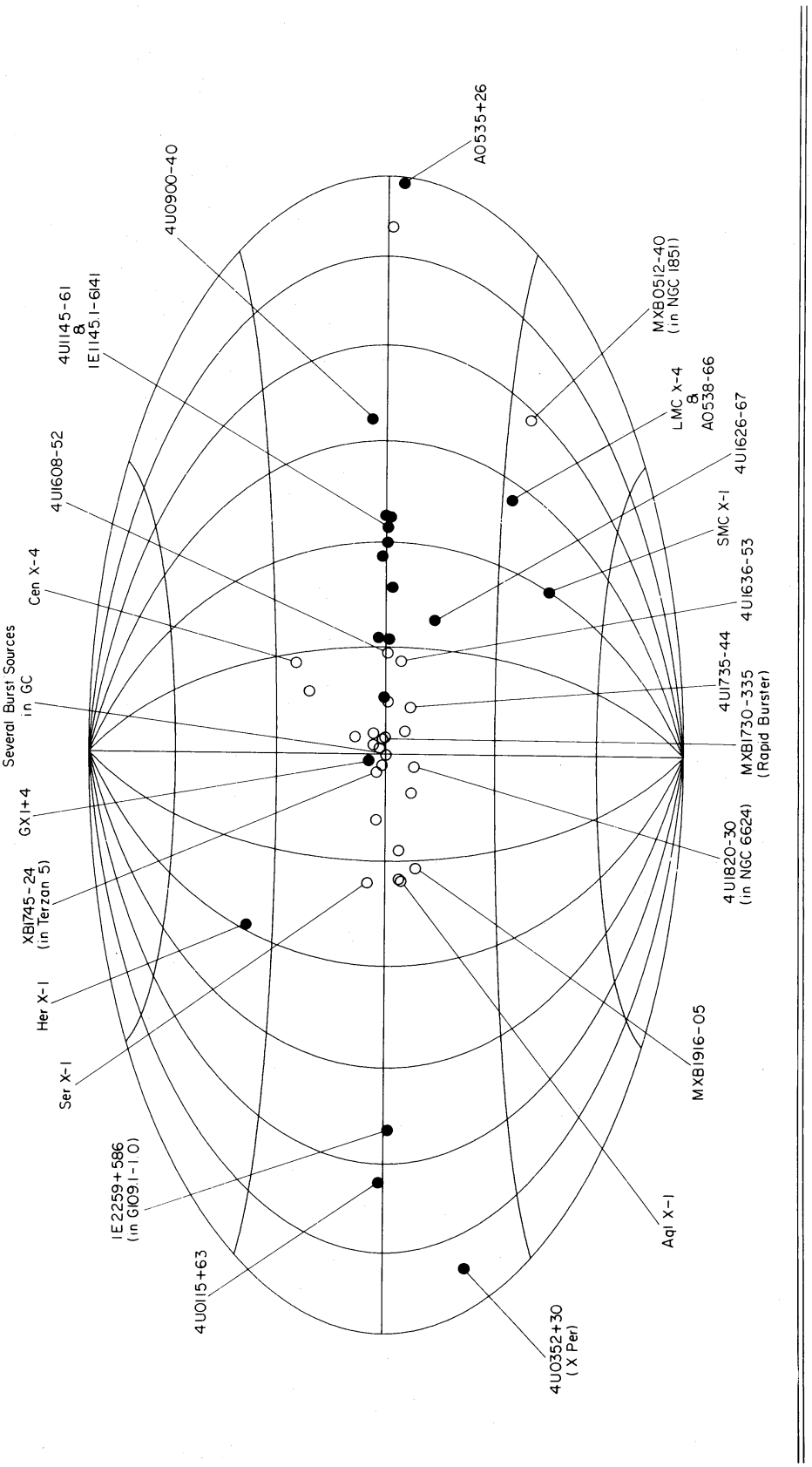


© Cambridge University Press • Provided by the NASA Astrophysics Data System

© Cambridge University Press • Provided by the NASA Astrophysics Data System

Source	Optical counter-part	Pulse period (s)	$-\dot{P}/P$ (yr^{-1})	Orbital period (d)	$a_x \sin i$ (lt-s)	$f(M)$ ($M_\odot$)	Orbital eccen-tricity	K_c[a] (km s^{-1})	Eclipse half-angle (°)	L_x[b] (erg s^{-1})
A 0538−66	Identified	0.069	—	16.66	—	—	>0.4	—	—	1.2×10^{39}
SMC X−1	Sk 160	0.714	7.1×10^{-4}	3.892	53.46(3)	10.8	<0.0007	19(2)	26.5–29	6×10^{38}
Her X−1	HZ Her	1.24	2.9×10^{-6}	1.700	13.1831(3)	0.85	<0.0003	20.2(3.5)	24.4–24.7	7×10^{36}
1E 2259+586	Identified	3.49	—	<0.08	—	—	—	—	—	3×10^{34}
4U 0115+63	Identified	3.61	3.2×10^{-5}	24.31	140.13(10)	5.00	0.3402(2)	—	0	8×10^{36}
Cen X−3	V779 Cen	4.84	2.8×10^{-4}	2.087	39.792(5)	15.5	0.0008(1)	24(6)	35–40	8×10^{37}
4U 1626−67	KZ TrA	7.68	1.9×10^{-4}	0.0288	<0.04	$<8 \times 10^{-5}$	—	280(76)	0	—
2S 1553−54	—	9.26	—	30.7(2.8)	165(30)	5.1(2.9)	<0.07	—	—	—
LMC X−4	Identified	13.5	$<1.2 \times 10^{-3}$	1.408	30(5)	15(8)	<0.2	37.9(2.4)	25.5–33	4×10^{38}
2S 1417−62	—	17.6	9×10^{-3} (?)	>15	>25	—	—	—	—	—
OAO 1653−40	—	38.2	5.4×10^{-3}	—	—	—	—	—	—	—
A 0535+26	HDE 245770	104	3.5×10^{-2}	111(?)	—	—	—	$\lesssim 20$	—	2×10^{37}
GX 1+4	V2116 Oph	122	2.1×10^{-2}	>15	>60	—	—	—	—	6×10^{37}
GX 304−1	Identified	272	—	132(?)	—	—	—	—	—	3×10^{36}
4U 0900−40	HD 77581	283	1.7×10^{-4}	8.965	113.0(8)	19.3	0.092(5)	21.8(1.2)	31–37	6×10^{36}
4U 1145−61	HEN 715	292	$<10^{-4}$	187(?)	>100	—	—	—	—	6×10^{36}
1E 1145.1−6141	Identified	297	$<10^{-4}$	>12	>50	—	—	—	—	3×10^{36}
A 1118−61	HEN 3−640	405	—	—	—	—	—	—	—	5×10^{36}
4U 1538−52	QV Nor	529	$<2 \times 10^{-3}$	3.730	55.2(3.7)	13	—	33(7)	25–33	4×10^{36}
GX 301−2	WRA 977	696	7×10^{-3}	41.4	367(3)	31	0.47(1)	—	0	1×10^{37}
4U 0352+30	X Per	835	1.8×10^{-4}	580(?)	—	—	—	<20	—	1×10^{34}

[a] K_c = semiamplitude of the optical Doppler velocity curve.
[b] L_x = X-ray luminosity (2–11 keV) from Bradt, H. & McClintock. *Ann. Rev. Astron. Astrophys.*, **21**, 13, 1983.
(Adapted from Joss, P. C. and Rappaport, S. A., *Ann. Rev. Astron. Astrophys.*, **22**, 537, 1984.)



Sky map, in galactic coordinates, of 21 binary X-ray pulsars (●) and 27 X-ray burst sources (○). (Reproduced, with permission, from the *Annual Review of Astronomy and Astrophysics*, Vol. 22, © 1984, by Annual Reviews Inc. Courtesy of Paul C. Joss, MIT.)

© Cambridge University Press • Provided by the NASA Astrophysics Data System

X-ray emitting supernova remnants

Source	α 1950 δ 1950	Distance (kpc)	Diameter (pc)	L_x (0.2–2 keV) (10^{35} erg s^{-1})	Age (yr)	1 GHz flux density (fu)	Angular size (arcmin)
Crab Nebula	$05^h\,31^m$ $21°\,59'$	2	3	160	900	1000	3.0 × 4.2
Cas A	23 21 58 33	3	3.5	30	300	3000	4.0 × 3.8
Cygnus Loop	20 49 30 30	0.8	40	8	20 000	180	200 × 160
Vela	8 32 −45 00	0.5	44	4	13 000	1800	220 × 180
IC 443	06 14 22 30	1.5	20	0.4	6000	160	40 diameter
Tycho's SNR	00 22 63 52	6	13	40	400	58	6.0 × 7.0
SN 1006	15 00 −41 45	1.2	10	0.2	970	25	30 × 22
GKP SNR	19 31 31 10	1.2	70	0.8	300 000	50	240 × 200
Lupus Loop	15 09 −40	0.5	40	0.1	20 000	340	270 diameter
RCW 86	14 39 −62 15	2.5	28	2	1800	33	40 diameter
RCW 103	16 14 −50 56	3.3	9	1	1000	22	7.0 × 7.9
PKS 1209−52	12 06 −52 10	2	40	0.7	20 000	49	86 × 75
Pup A	08 20 −42 50	1.2	17	6	10 000	145	55 diameter
65.6+6.5	19 31 31 10	1.2	60–80	0.7	$< 2 \times 10^4$		180 × 240

© Cambridge University Press • Provided by the NASA Astrophysics Data System

Crab Nebula

The observed electromagnetic spectrum of the Crab Nebula and the Crab Pulsar. Dashed lines show corrections made for absorption and scattering of interstellar material. (Adapted from Seward, F. O., *Journal of the British Interplanetary Society*, **31**, 83, 1978.)

X-ray spectrum (0.1–100 keV):

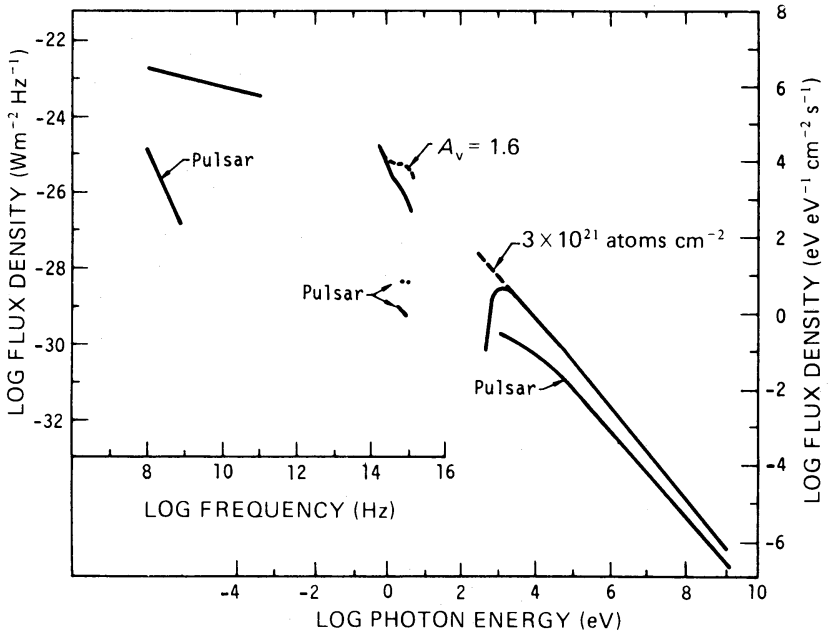
$$\frac{dN}{dE} = 10\,E^{-2.05}\exp(-\sigma n_H)\ \text{photons cm}^{-2}\,\text{s}^{-1}\,\text{keV}^{-1},$$

$$n_H = 3 \times 10^{21}\ \text{cm}^{-2}.$$

X-ray luminosity (0.1–100 keV):

$$L_x = 4.9 \times 10^{37}\ \text{erg s}^{-1}$$

Distance:	2200 pc
Diameter:	3 pc (5 arcmin)
m_v:	8.6
A_v (absorption):	1.5
Coordinates:	$\alpha = 05^h31^m$, $\delta = +22°$
Total radiated energy:	1.8×10^{38} erg s^{-1}
Age:	900 years (AD 1054)
Pulsar period, P(1969):	0.0331 s
Rate of period increase, $\dot{P}$:	422.69×10^{-15} ss^{-1}.



© Cambridge University Press • Provided by the NASA Astrophysics Data System

X-ray emission from normal galaxies

Galaxy	Distance (Mpc)	Radius (kpc)	Total mass ($10^{10}\,M_\odot$)	X-ray luminosity[a] (2–10 keV) (erg s^{-1})	L_x/M (erg s^{-1} $M_\odot^{-1}$)
LMC	0.052	3.5	1.0	4×10^{38}	4×10^{28}
SMC	0.063	1.5	0.15	1×10^{38}	6×10^{28}
M31	0.67	8	30	3×10^{39}	1×10^{28}
Our Galaxy		12	14	5×10^{39}	4×10^{28}

X-ray emission from clusters of galaxies

Cluster	Distance (Mpc)	Radius (Mpc)	Optical luminosity ($10^{11}\,L_\odot$)	Virial mass / Luminosity ($M_\odot/L_\odot$)	X-ray luminosity[a] (2–10 keV) (erg s^{-1})
Perseus	97	0.44	10.0	461	1×10^{45}
Coma	113	2.63	49.0	1020	5×10^{44}
Centaurus	250				4×10^{43}
Virgo	19	1.07	12.0	668	1.5×10^{43}

X-ray emission from active galaxies

Object	Class of galaxy	X-ray source	2–10 keV flux density (10^{-11} erg cm^{-2} s^{-1})	D[b] (Mpc)	X-ray luminosity[a] (2–10 keV erg s^{-1})
NGC 4151	Seyfert	4U 1206+39	10	20	5×10^{42}
Cen A	Giant radio source	4U 1322−42	20	9	2×10^{42}
3C 273	Quasar	4U 1226+02	6	950	7×10^{45}
M87	Radio source in cluster	4U 1228+12	52	25	4×10^{43}
NGC 1275 (Perseus A)	Peculiar Seyfert in cluster	4U 0316+41	29	110	4×10^{44}
3C 120	Radio/optical variable, Seyfert	4U 0432+05	7	190	3×10^{44}
3C 390.3	N galaxy, compact radio source	4U 1847+78	7	336	1×10^{45}
M82	Emission line galaxy	4U 0954+70	6	4	1×10^{41}
Mkn 501	BL Lac object	4U 1651+39	5	180	2×10^{44}

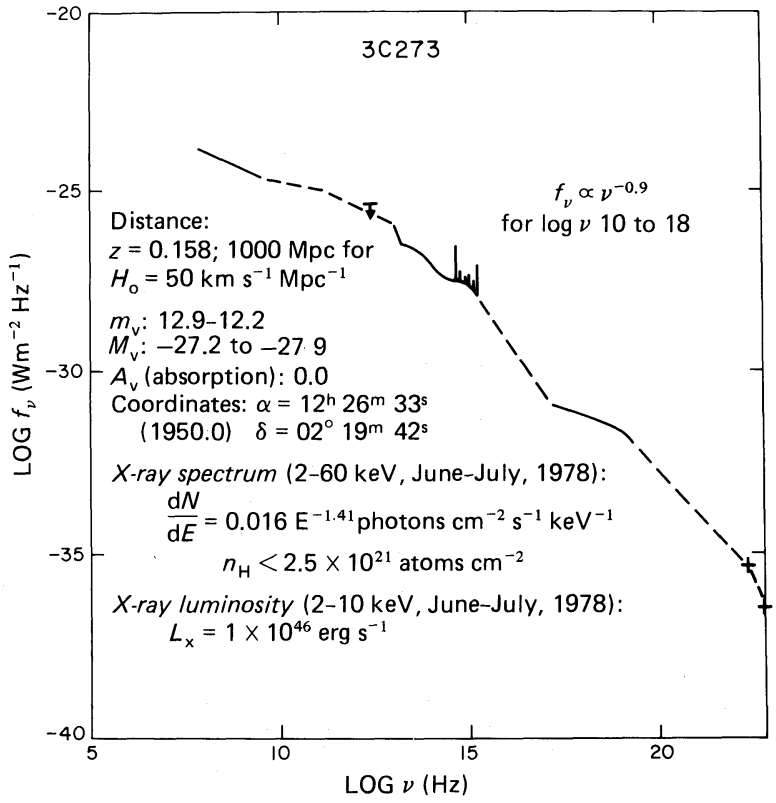
[a] $L_x = (\text{X-ray flux})\cdot 4\pi D^2$.

[b] $D = \dfrac{zc}{H_0}$ $(H_0 = 50\ \text{km s}^{-1}\ \text{Mpc}^{-1})$.

© Cambridge University Press • Provided by the NASA Astrophysics Data System

3C 273

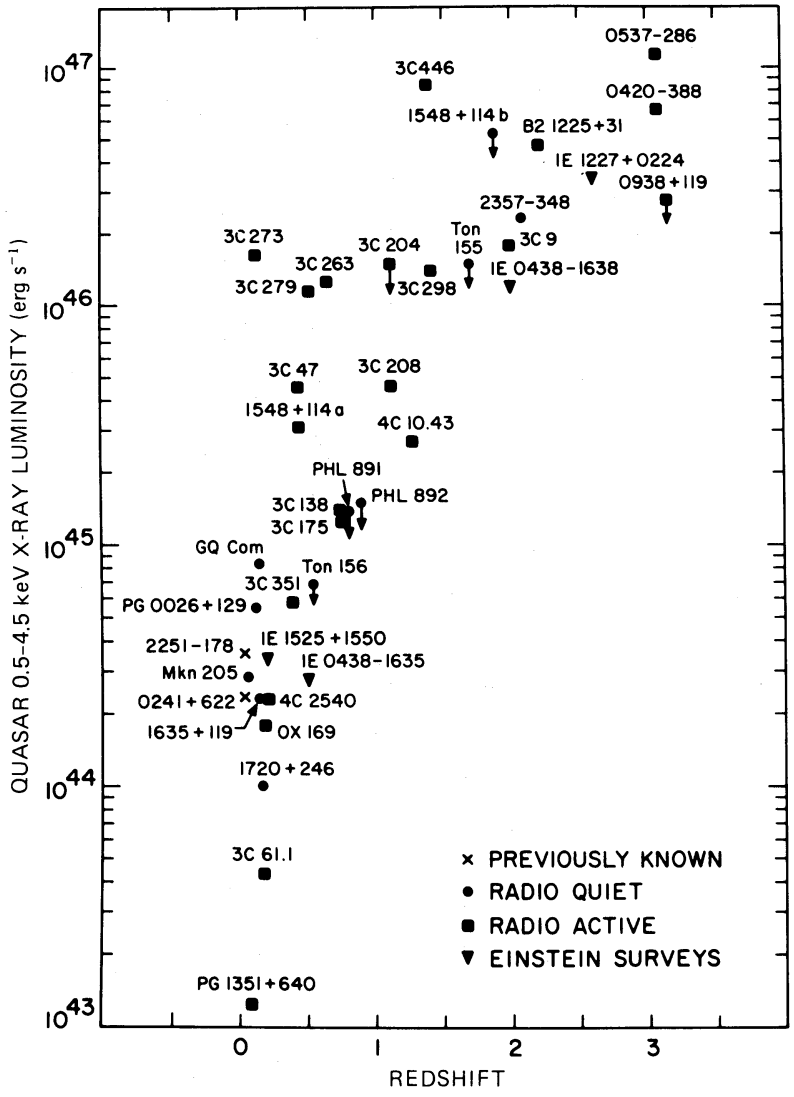
The observed electromagnetic spectrum of the quasar 3C273 (3C273 is variable). (From Worrall, D. M. *et al.*, *Ap. J.*, **232**, 683, 1979.)



© Cambridge University Press • Provided by the NASA Astrophysics Data System

Quasar X-ray luminosity

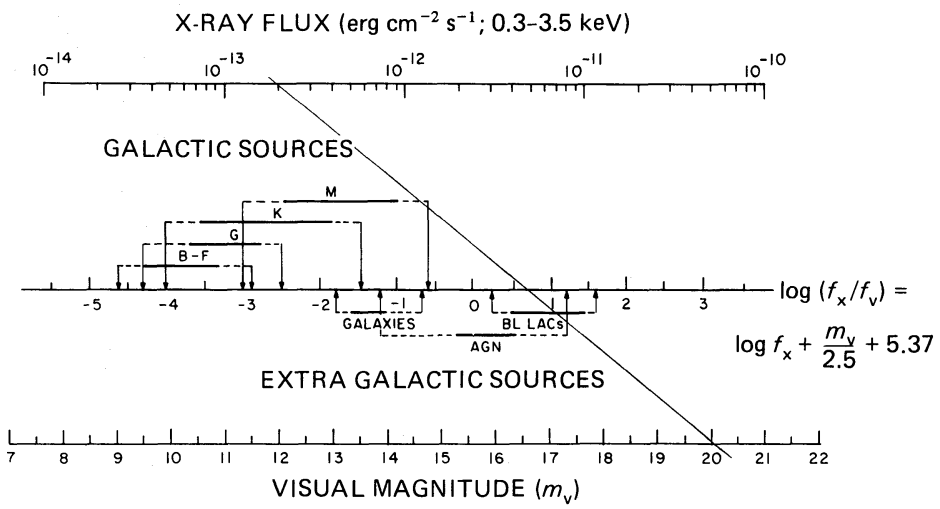
Quasar X-ray luminosity (0.5–4.5 keV) versus redshift. (Courtesy H. Tananbaum, Harvard/Smithsonian Center for Astrophysics.)



© Cambridge University Press • Provided by the NASA Astrophysics Data System

X-ray source nomogram

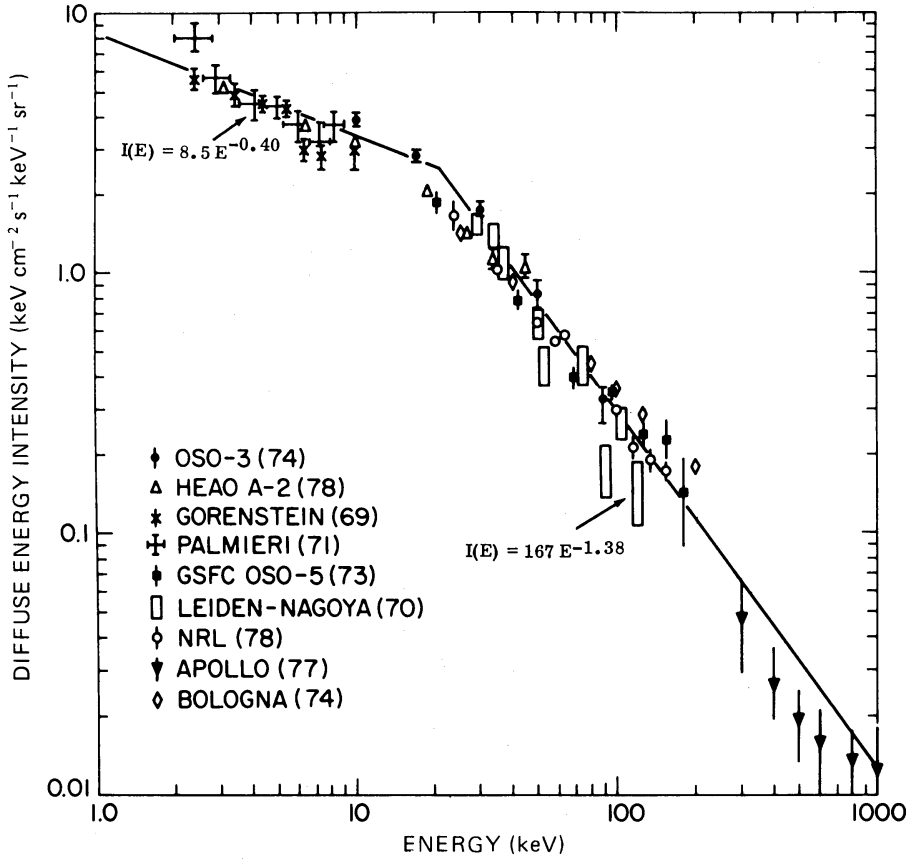
Nomogram to compute $\log(f_x/f_v)$ for X-ray sources, where f_x is the X-ray flux density in erg cm^{-2} s^{-1} in the 0.3–3.5 keV band and f_v is the flux density in the V band. For each object class indicated (stars: B–F, G, K, M; normal galaxies; active galactic nuclei; BL Lac objects) a continuous horizontal line indicates the range of $\log(f_x/f_v)$ comprising 70% of the known sources in the class and a dashed line indicates the range comprising the highest and lowest 15% of the sources. For example, for an X-ray source with a flux density of 2×10^{-13} erg cm^{-2} s^{-1} and a V magnitude of 20, $\log(f_x/f_v)$ is ~ 0.7 and the source is most likely a BL Lac object. (From Maccacaro, T. *et al.*, *Ap. J.*, **326**, 680, 1988).



© Cambridge University Press • Provided by the NASA Astrophysics Data System

Diffuse X-ray background

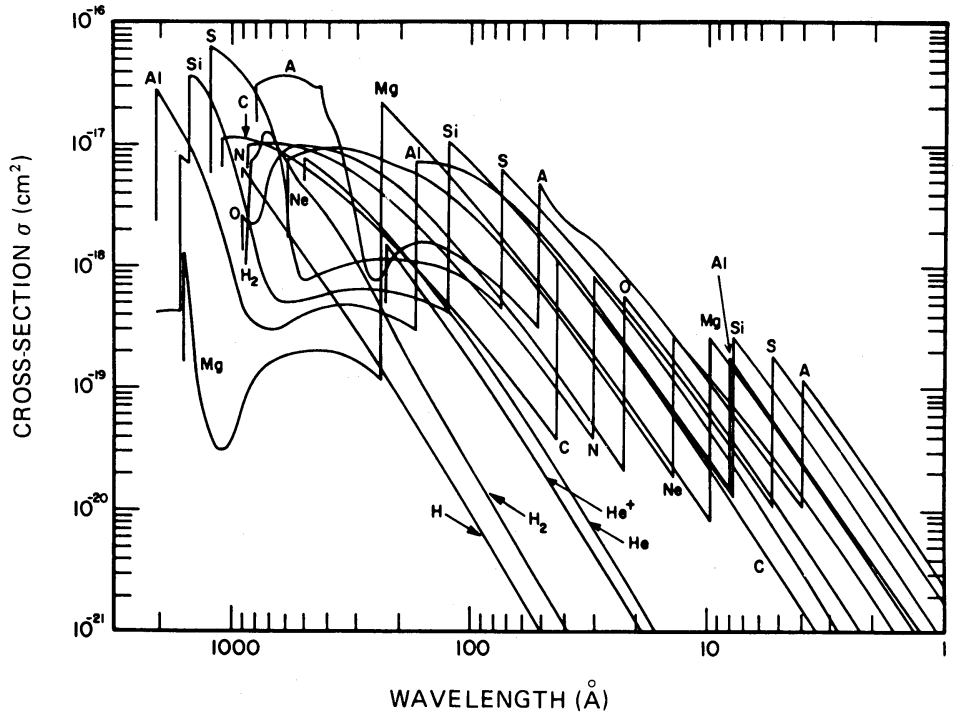
Energy spectrum of diffuse X-ray background. (Courtesy of D. Schwartz, Harvard/Smithsonian Center for Astrophysics.)



© Cambridge University Press • Provided by the NASA Astrophysics Data System

Photoabsorption cross-sections (UV–X-ray) of abundant elements

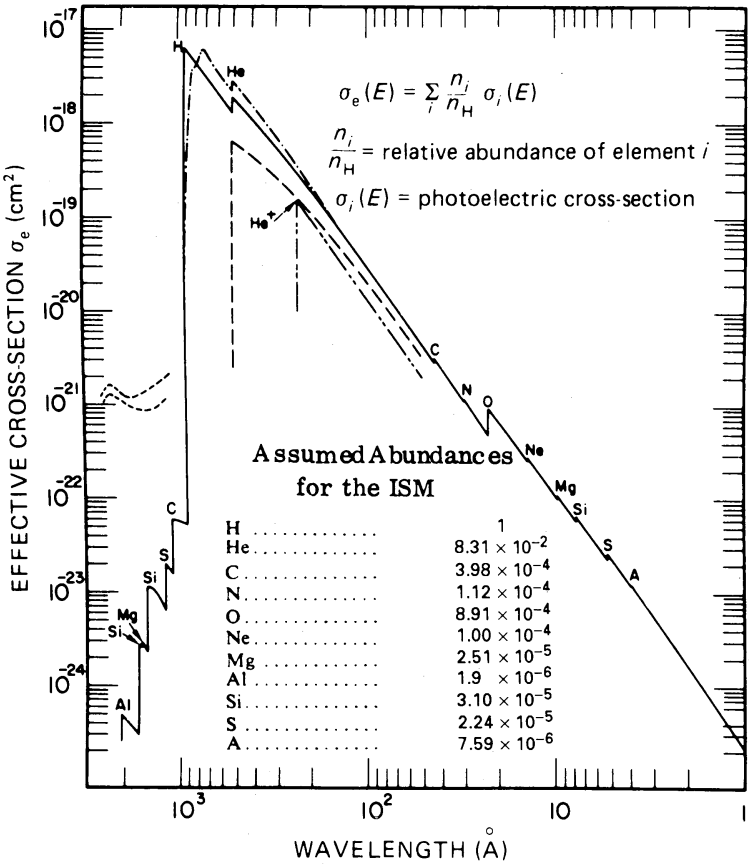
Photoabsorption cross-sections of the abundant elements in the interstellar medium as a function of wavelength. (Adapted from Cruddace, R., Paresce, F., Bowyer, S. & Lampton, M., *Ap. J.*, **187**, 497, 1974.)



© Cambridge University Press • Provided by the NASA Astrophysics Data System

Effective cross-section of the interstellar medium

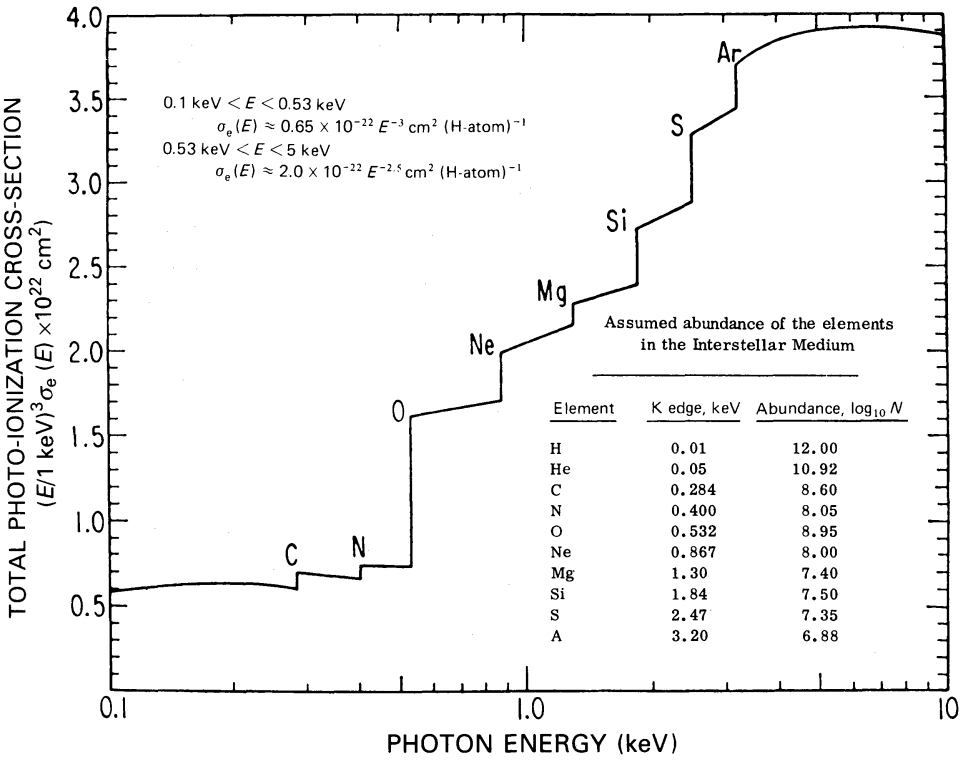
Effective cross-section (cross-section per hydrogen atom or proton) of the interstellar medium: —— gaseous component with normal composition and temperature; –·– hydrogen, molecular form; —— HII region about a B star; ——— HII region about an O star; ———— dust. (Adapted from Cruddace, R., Paresce, F., Bowyer, S. & Lampton, M., *Ap. J.*, **187**, 497, 1974.)



© Cambridge University Press • Provided by the NASA Astrophysics Data System

Total photoionization cross-section

Total photo-ionization cross-section per hydrogen atom $[x(E/1\,\text{keV})^3]$ in units $10^{-22}\,\text{cm}^2$ as a function of incident photon energy for a gas having a cosmic elemental abundance. The elements responsible for the discontinuities due to their K edges are shown. (Adapted from Brown, R. L. & Gould, R. J., *Physical Review*, **01**, 2252, No. 8, 1970.)

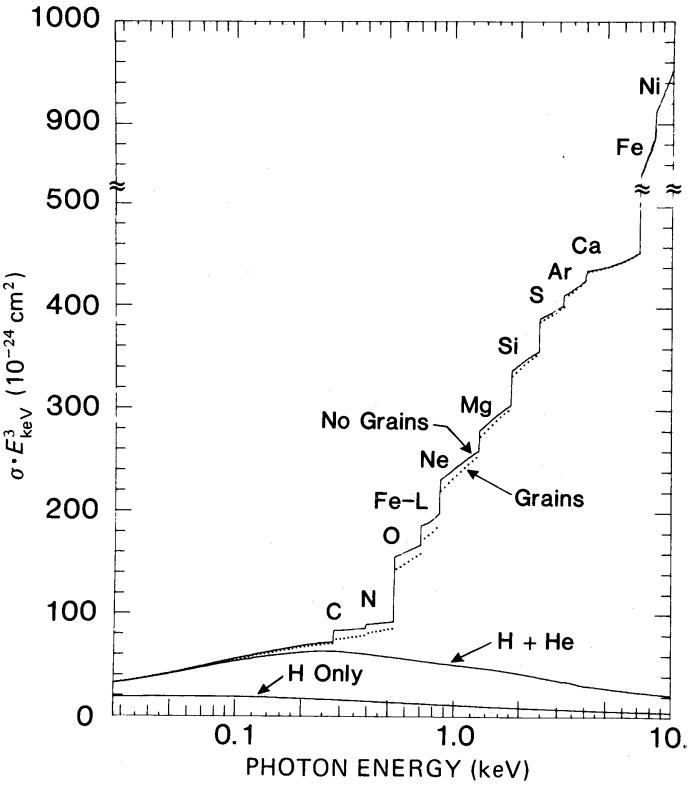


Element	K edge, keV	Abundance, $\log_{10} N$
H	0.01	12.00
He	0.05	10.92
C	0.284	8.60
N	0.400	8.05
O	0.532	8.95
Ne	0.867	8.00
Mg	1.30	7.40
Si	1.84	7.50
S	2.47	7.35
A	3.20	6.88

© Cambridge University Press • Provided by the NASA Astrophysics Data System

Photoelectric absorption cross-section

Net photoelectric absorption cross-section per hydrogen atom as a function of energy, scaled by $(E/1\,\mathrm{keV})^3$. The solid line is for relative abundances given in the table of elemental abundances below, with all elements in the gas phase and in neutral atomic form. The dotted line shows the effect of condensing the fraction of each element indicated in the table into 0.3 μm grains. The contributions of hydrogen and hydrogen plus helium to the total cross-section are also shown. (From Morrison, R. & McCammon, D., *Ap. J.*, **270**, 119, 1983. Diagram courtesy of D. McCammon.)



© Cambridge University Press • Provided by the NASA Astrophysics Data System

Elemental abundances

Element	Abundance[a]	Fraction in grains[b]
H	12.00	0
He	11.00	0
C	8.65	1
N	7.96	1
O	8.87	0.25
Ne	8.14	0
Na	6.32	1
Mg	7.60	1
Al	6.49	1
Si	7.57	1
S	7.28	1
Cl	5.28	1
Ar	6.58	0
Ca	6.35	1
Cr	5.69	1
Fe	7.52	1
Ni	6.26	1

[a] Log_{10} abundance relative to hydrogen = 12.00. All values except helium are from Anders and Ebihara, 1982.

[b] Fraction of atoms of each element assumed depleted from gas phase and condensed into grains of average thickness 2.1×10^{18} atoms cm^{-2} for case shown as dotted line in the diagram.

Coefficients of analytic fit to cross-section

Energy range (keV)	c_0	c_1	c_2
0.030–0.100[a]	17.3	608.1	−2150
0.100–0.284	34.6	267.9	−476.1
0.284–0.400	78.1	18.8	4.3
0.400–0.532	71.4	66.8	−51.4
0.532–0.707	95.5	145.8	−61.1
0.707–0.867	308.9	−380.6	294.0
0.867–1.303	120.6	169.3	−47.7
1.303–1.840	141.3	146.8	−31.5
1.840–2.471	202.7	104.7	−17.0
2.471–3.210	342.7	18.7	0.0
3.210–4.038	352.2	18.7	0.0
4.038–7.111	433.9	−2.4	0.75
7.111–8.331	629.0	30.9	0.0
8.331–10.000	701.2	25.2	0.0

Note: cross-section per hydrogen atom $= (c_0 + c_1E + c_2E^2)E^{-3} \times 10^{-24}\,\mathrm{cm}^2$ (E in keV).

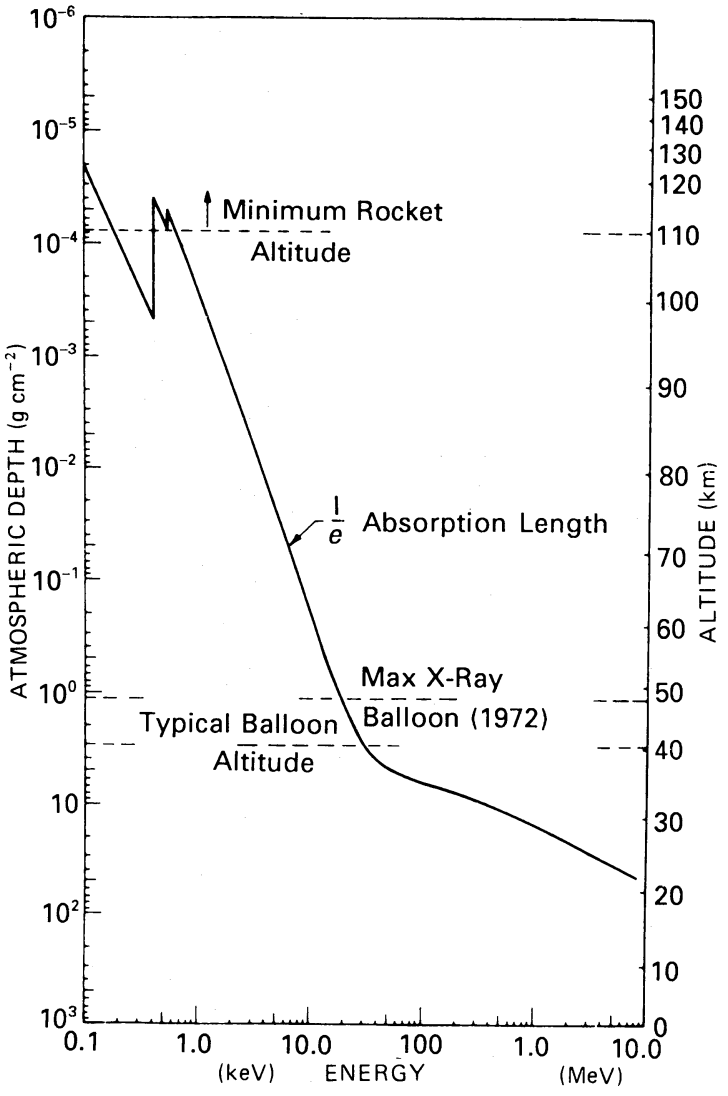
[a] Break introduced to allow adequate fit with quadratic: no absorption edge at 0.1 keV.

(From Morrison, R. & McCammon, D., *op. cit.*)

© Cambridge University Press • Provided by the NASA Astrophysics Data System

Attenuation of photons in the atmosphere

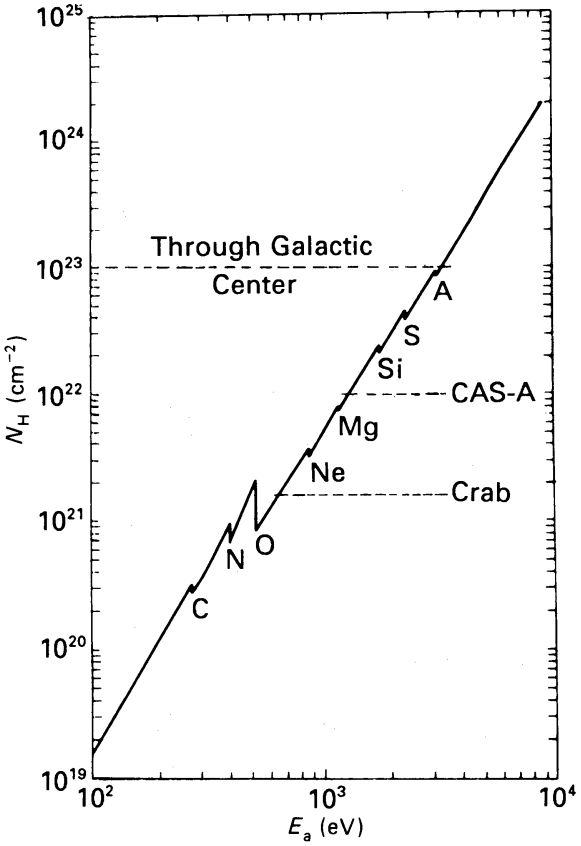
Attenuation of photons in the 1972 COSPAR International Reference Atmosphere with $1/e$ absorption length plotted as a function of energy and altitude or atmospheric depth.



© Cambridge University Press • Provided by the NASA Astrophysics Data System

Photoelectric absorption in the interstellar medium

Photoelectric absorption in the interstellar medium. The vertical axis gives the column density in units of hydrogen atoms cm^{-2} at which the absorption is $1/e$ at the photon energy E_a. (For a hydrogen atom number density of $1/cm^3$. 1 kpc is equivalent to a column density of 3.1×10^{21} hydrogen atoms cm^{-2}.)



An incomplete list of astrophysically important X-ray spectral features

Identification	Energy (keV)†	Identification	Energy (keV)†
Ne VII	0.127	N VII	0.500
Si XI	0.283	O I K edge	0.532
C I K edge	0.284	O VII	0.569
Si XII	0.303	O VII	0.574
C V	0.308	O VIII	0.654
N I K edge	0.402	O VII	0.666
N VI	0.431	O VII	0.698

© Cambridge University Press • Provided by the NASA Astrophysics Data System

continued

Identification	Energy (keV)†	Identification	Energy (keV)†
Fe I LIII edge	0.707	Si XIII	1.86
Fe I LII edge	0.721	S I K edge	2.472
Fe XVII	0.826	Ar I K edge	3.203
Ne I K edge	0.867	Fe I $K\alpha_2$	6.391
Ne IX	0.915	Fe I $K\alpha_1$	6.404
Ne IX	0.922	Fe XXV	6.64
Fe XX	0.996	Fe XXV	6.68
Ne X	1.022	Fe XXV	6.70
Mg I K edge	1.305	Fe XXVI	6.93
Mg XI	1.340	Fe I $K\beta$	7.058
Mg XI	1.352	Fe I K edge	7.111
Si K edge	1.839		

† λ (Å) = 12.399/E (keV).

Model X-ray spectral distributions for non-dispersive spectroscopy

$$f(E) = C\,\mathrm{e}^{-\sigma_e(E)N_H} f(S,E) \quad \text{photons cm}^{-2}\,\text{s}^{-1}\,\text{keV}^{-1},$$

where

C = normalization constant,

N_H = hydrogen column density to source,

$\sigma_e(E)$ = photoelectric cross-section per hydrogen atom for absorption of photons of energy E by interstellar medium. For $E > 3$ keV: $\sigma_e(E)N_H \approx (E_a/E)^{8/3}$, where E_a is a low energy cutoff parameter.

S is a parameter in the intrinsic spectral shape:

Thermal bremsstrahlung:

$$S = T, \quad f(S,E) = \overline{g(T,E)}\,\mathrm{e}^{-E/kT}/E(kT)^{1/2},$$

where $\overline{g(T,E)}$ is the temperature-averaged Gaunt factor.

Power law:

$$S = n, \quad f(S,E) = E^{-n}.$$

Blackbody:

$$S = T, \quad f(S,E) = E^2/(\mathrm{e}^{+E/kT} - 1).$$

For optically identified sources:

$$N_H \approx (2.22 \pm 0.3) \times 10^{21} A_v \quad \text{cm}^{-2}\,\dagger$$

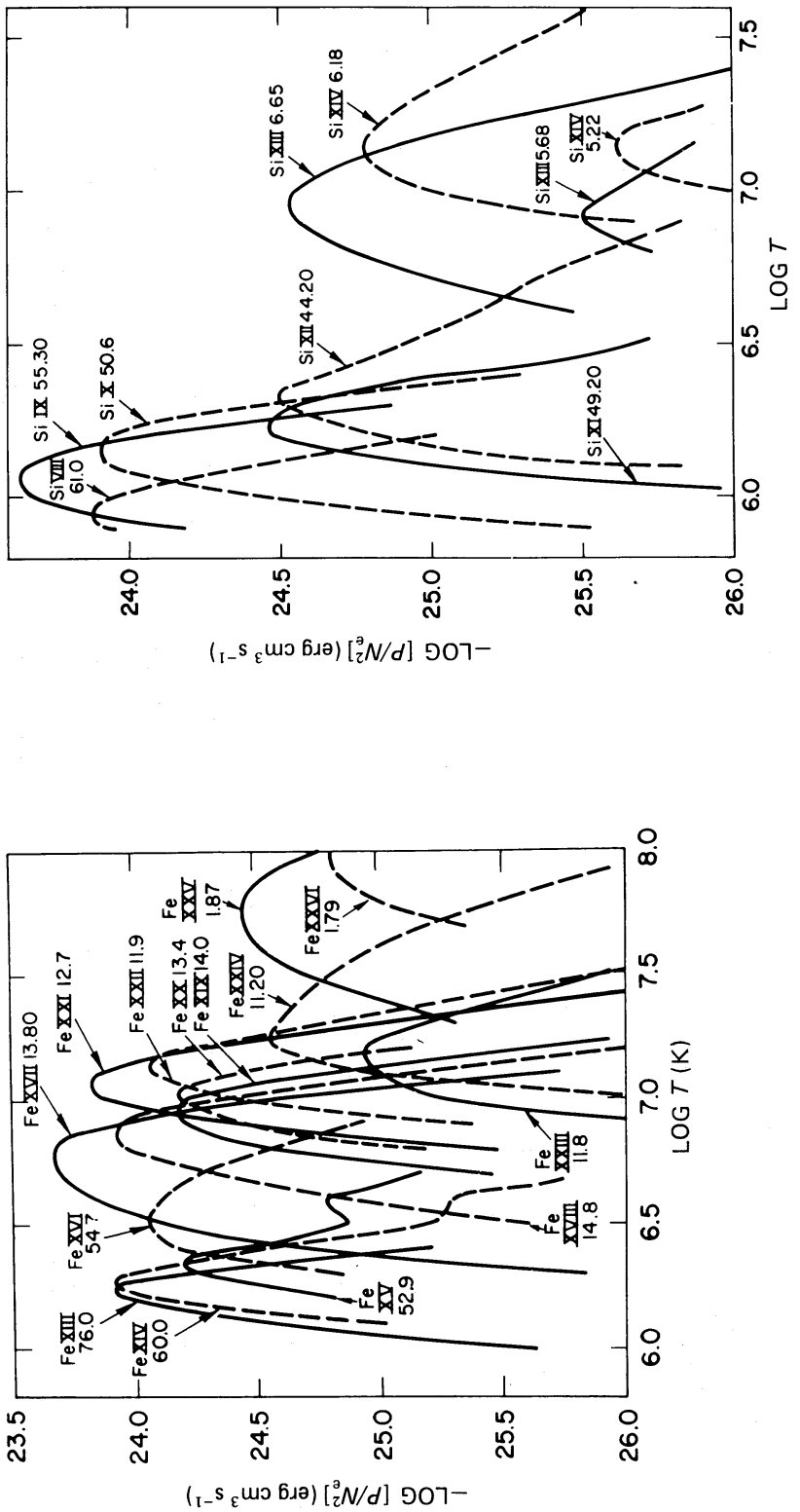
$$A_v = 3.0 E_{B-V} \quad \text{(color excess)}.$$

† (Gorenstein, P., *Ap. J.*, **198**, 40, 1975.)

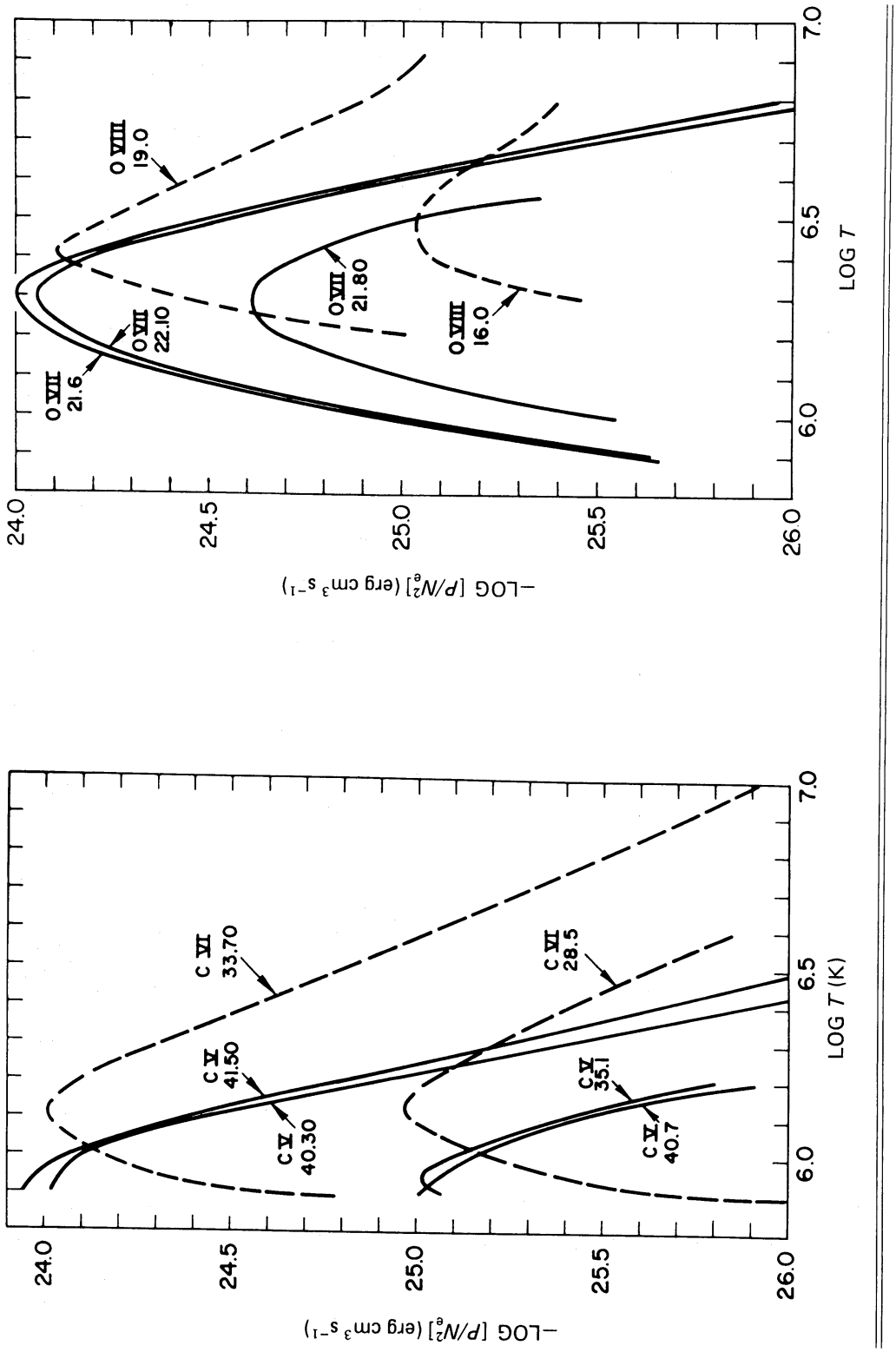
© Cambridge University Press • Provided by the NASA Astrophysics Data System

Emission lines for low density plasma

Power per unit emission integral for some of the strong emission lines for a low density plasma as a function of temperature. Elemental abundances characteristic of the solar corona have been assumed: A ($\log N$) = H (12.00), He (11.30), C (8.70), O (8.50), Ne (7.60), Mg (7.50), Si (7.70), S (7.30), Ca (6.30), Fe (7.70), and Ni (6.70). (Adapted from Tucker, W. H. and Blumenthal, G. R. in *X-ray Astronomy*, R. Giacconi & H. Gursky, eds., D. Reidel Publishing Co., Dordrecht, 1974.)



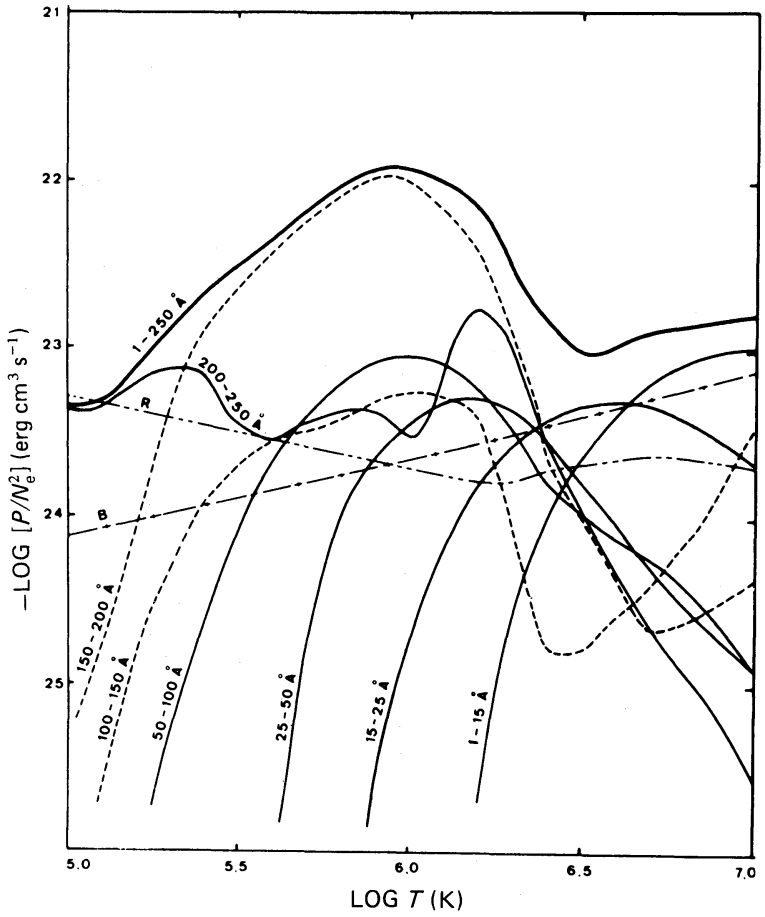
© Cambridge University Press • Provided by the NASA Astrophysics Data System



© Cambridge University Press • Provided by the NASA Astrophysics Data System

Plasma emission – power in lines

The power in lines radiated in various wavelength bands as a function of temperature for a low density plasma. Elemental abundances characteristic of the solar corona have been assumed. The power radiated in Bremsstrahlung (B) and radiative recombination (R) is also shown. (Adapted from Kato, T., *Ap. J. Suppl.*, **30**, 397, 1976.)



Bibliography

X-ray Astronomy, R. Giacconi & H. Gursky, eds., D. Reidel Publishing Co., 1974.

'Soft X-ray spectrum of a hot plasma', Raymond, J. C. & Smith, B. W., *Ap. J. Suppl.*, **30**, 419 (1977).

'Radiation from a hot, thin plasma from 1 to 250 Å', Kato, T., *Ap. J. Suppl.*, **30**, 397 (1976).

'Radiation from a high-temperature, low-density plasma: the X-ray spectrum of the solar corona', Tucker, W. H. & Koren, M., *Ap. J.*, **168**, 283 (1971).

© Cambridge University Press • Provided by the NASA Astrophysics Data System

'Calculated solar X-radiation from 1 to 60 Å', Mewe, R., *Solar Phys.*, **22**, 459 (1972).
'Calculated solar X-radiation', Mewe, R., *Solar Phys.*, **44**, 383 (1975).

© Cambridge University Press • Provided by the NASA Astrophysics Data System

© Cambridge University Press • Provided by the NASA Astrophysics Data System